Proceedings of the 19th World Congress
The International Federation of Automatic Control
Cape Town, South Africa. August 24-29, 2014

Performance Indices for Evaluation and Comparison of Unmanned Marine Vehicles' Guidance Systems

Eleonora Saggini [*,**] **Enrica Zereik** [*] **Marco Bibuli** [*]
Gabriele Bruzzone [*] **Massimo Caccia** [*] **Eva Riccomagno** [**]

[*] *CNR-ISSIA, Genova, Italy (e-mail: eleonora.saggini@ge.issia.cnr.it)*
[**] *UNIGE-DIMA, Genova, Italy*

Abstract: Guidance and control system development for Unmanned Marine Vehicles is a well known and consolidated issue, but a general guideline for quantitatively measuring the performance of robotic systems and comparing them is still lacking in the literature. The importance of establishing standards to follow has become more and more stronger, in particular whenever heterogeneous platforms are employed in a common framework. This work focuses on the definition and exploitation of performance indices for marine robotics applications, paying special attention to path-following tasks. Theoretical formalisations for the considered indices, as well as experimental results proving their effectiveness, are reported.

1. INTRODUCTION

Robotics is gradually becoming part of our daily life, starting from the first and simplest applications (e.g. domotics, assistance robotics, ...). Foreseeing a context where both robots and humans are present, it is absolutely necessary to be able to assess robotic systems' performances (e.g. to ensure safety, reliability and effectiveness) according to actual and significant criteria. From such considerations, the need to establish common evaluation indices and to spread them among the robotic community arises.

In particular, within the marine context, the application of such metrics allows the comparison of different architectures and robots, detecting the effectiveness of a specific algorithm with respect to another and, when teams from different institutions work together (e.g. within European projects), the objective and quantitative evaluaion of the project overall performances. Broadly speaking, good methodologies and standard guidelines for the design of experiments are needed in the field of marine robotics, being this last very affected by experimental constraints such as controllability of the conditions (e.g. waves, sea currents, recreational and commercial traffic), restricted number of executable experiments (due to cost and logistic issues), uncertainty in the robot inputs (as, due to hydrodynamic interactions, forces and torques assigned to the system are known with uncertainty). Moreover, the assessment of a control algorithm can be helpful for the experimenter to conduct a field trial and to notice possible unusual responses, due for example to heavy disturbances or mechanical damages.

Up to now there are very few works in literature dealing with this kind of problems; preliminary guidelines can be found in Bonsignorio et al. [2008], but they are only indications on how to write good experimental papers, not directly on how to design experiments. The importance of other related issues, such as the possibility to replicate experiments already conducted by other researchers, thus comparing the results, and to employ available data sets as well as common testing frameworks, is addressed in Amigoni et al. [2009], Bonsignorio et al. [2009] and Amigoni et al. [2007].

The main challenges in marine robotics are listed in Caiti [2011], where the author highlights the importance of having a credible measurement for algorithms' performance versus the costs needed for the organization of sea trials (many data should be collected in as many tests while evaluating an approach performance). The problem on how to evaluate the performance of a robot in a search and rescue context is faced in Tadokoro and Jacoff [2011] and Balakirsky et al. [2006], where the difficulty to evaluate system performance, due to several possible interpretations of the problem solution, is underlined.

Preliminary work by the present paper authors on good experimental methodologies for UMVs is reported in Caccia et al. [2013], in which some preliminary evaluation metrics are proposed; earlier work on evaluating path following algorithms can be found in Caccia et al. [2012] and Bibuli et al. [2009]. Constraints and limitations in field experiments (as already suggested above) are treated in Mišković et al. [2011] and Caccia et al. [2008c], in which repeatable experiments for ROV and USV identification have been conducted. Finally, methods for automatic detection of steady state conditions based on time series analysis have been recently proposed in Saggini [2012]. In this paper the authors address the specific task of path-following, providing standards to identify different phases in a typical line-following manoeuvre and introducing indices to evaluate both accuracy and efficiency of a control architecture. In Section 2, the problem statement is introduced, classifying the different phases of a path following experiment, while in Section 3 some proposed evaluation indices are formal-

⋆ This work has been supported by the EU FP7 MORPH (Marine robotic system of self-organizing, logically linked physical nodes) project, grant agreement no. 288704

ized. Then, in Section 4 two different path following algorithms that have been evaluated exploiting the introduced indices, are described; many experimental results about such different control schemes are reported in Section 5, together with a brief description of the experimental setup. Finally, some conclusions are drawn in Section 6, together with the plan for future work in the field of developing good experimental methodologies.

2. PROBLEM STATEMENT

As mentioned above a set of performance indices to measure the vehicle capability to follow a desired path is defined in the paper. In order to quantify at best the vehicle performance, different indices have been defined, depending on the position and orientation of the vehicle with respect to the target path. To this aim the robot overall manoeuvre is divided into four phases (delimited by P_1, P_2 and P_3), as shown in Figure 1:

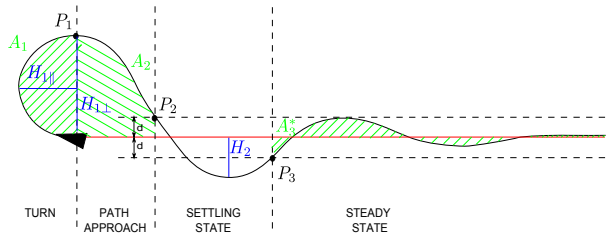

Fig. 1. Classical path-following manoeuvre with different phases and relative indices adopted for the performance evaluation of path-following guidance systems.

(1) *Turn*: the vehicle starts adjusting its position and orientation in order to properly approach and follow the desired path. Usually in this phase the cross-track error increases; this is true except for the case $\psi \notin (\psi^* - 90°, \psi^* + 90°)$, where ψ^* is the angle characterizing the target line and ψ is the initial heading, in which the cross-track error firstly decreases before starting to increase. Within a lawn mowing pattern, for example, the turn phase starts each time that the vehicle has to change its motion direction and ends whenever the cross-track error starts decreasing and $\psi \in (\psi^* - 90°, \psi^* + 90°)$. It is worth noting that, within a general path following execution, the turn phase could be skipped, because of its strong dependence on the vehicle initial position and orientation.
(2) *Path Approach*: the vehicle moves towards the desired path. Unlike the previous phase, during the path approach the cross-track error can only decrease. This phase starts at the end of the turn and lasts until the distance between the vehicle and the target path is below a predefined value d.
(3) *Settling State*: the vehicle is close to the path but it is still oscillating around the final desired value. This third phase lasts until the distance from the path is greater than d.
(4) *Steady State*: the vehicle motion stabilizes around the desired path, i.e. the distance between the vehicle and the path never exceeds the value d and this condition is maintained for at least $\overline{s}$ seconds, where usually $\overline{s} = 20$. The steady state ends when the reference for a new path following manoeuvre is issued.

The diagram in Figure 2 shows the different possible connections among the phases. For example, recalling that a settling or steady state can be interrupted, then the vehicle can come back to the turn or the approach state until it stabilizes again on the path.

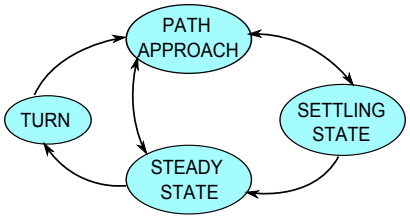

Fig. 2. Diagram showing the possible connections among the different phases.

3. EVALUATION INDICES

The accuracy and efficiency of the guidance system are measured exploiting different proposed quantities providing information that is, somehow, complementary. Thus the key idea consists in comparing the proposed indices to obtain a general evaluation for a specific control architecture. Being inspired by classic closed-loop performance measures (the overshoot and the integral absolute error are respectively connected to the Hausdorff distance and to the area index), a list of performance indices that focus on path-following tasks is formally expressed in the following.

3.1 Area

Aiming to quantitatively evaluate the accuracy of a path following execution, the area between the vehicle and target paths can be computed. Let $\{(x_{F,i}, y_{F,i}), i = 1, \ldots, n\}$ and $\{(x_{T,i}, y_{T,i}), i = 1, \ldots, m\}$ be the two sets of GPS coordinates identifying the follower and the target paths, respectively. The two paths can be thus regarded as two finite chain of straight line segments and the areas of non-self-intersecting and consecutive polygons can be easily computed, so that the indices A_1 and A_2 (refer to Figure 1) can be retrieved. Furthermore, in order to get an index evaluating the area in steady state (which does not depend on the experiment duration), the computed total area A_3 is normalized with respect to the target path length, leading to the normalized index A_3^*.
The main advantages of this method are represented by the possibility to compute these indices online, very accurately and in the most general situation, when a different number of samples is available (i.e. $n \neq m$) and the target path is not defined by a mathematical function.

3.2 Hausdorff distance

A well known metric, which is nowadays broadly employed in image matching and handwriting recognition applications, as well as its modified versions as in in Zhu et al. [2012] and Fischer et al. [2013], is the Hausdorff distance; it provides a measure of the maximum of all the distances from a point in one set to the closest point in the other set. More formally, the Hausdorff distance from a set A to a set B is defined as

$$H(A, B) = \max\{d_H(A, B), d_H(B, A)\}, \qquad (1)$$

where $d_H(A,B)$ is the directed Hausdorff distance from a set A to a set B, defined as

$$d_H(A,B) = \max_{a\in A}\{\min_{b\in B} d(a,b)\},$$

where d is the Euclidean distance. The definition (1) can be directly applied to the path following application context, where $A = \{(x_{F,i}, y_{F,i}), i = 1,\dots,n\}$ and $B = \{(x_{T,i}, y_{T,i}), i = 1,\dots,m\}$. Considering the above definition and recalling Figure 1, parameters $H_{1\perp}$ and H_2 can be directly computed as the distance between the target and the follower paths. For the $H_{1\parallel}$ index the computation is slightly different: the perpendicular line from point P_1 to the reference path is to be considered instead of the set B. Note that in the case represented in Figure 1 (straight line) the Hausdorff distance degenerates to a simple point-to-line distance; this is a particular case but in general the Hausdorff distance is useful to be applied to a more generic (curvilinear) path. With respect to the area value, this index penalises the case in which there are few error peaks with respect to the mean value.

3.3 Cross-track error decreasing rate

The cross-track error $X_{TE}(t)$, defined as the distance (along the direction normal to the path) between the actual vehicle position and the target path at time t, is considered in order to evaluate the system response speed during the path approach phase. The chosen indices are the mean and the maximum decreasing rate, defined as

$$\overline{\chi} = \frac{\sum_{t=1}^{T-1} |\Delta X_{TE}(t)|}{T} \quad \text{and} \quad \chi_{\max} = \max_{t=1,\dots,T-1} |\Delta X_{TE}(t)|,$$

where $\Delta X_{TE}(t) = X_{TE}(t+1) - X_{TE}(t)$ and T is obtained by multiplying the sampling rate ($[Hz]$) and the path approach duration ($[s]$).

3.4 Rudder stress

In addition to the precision indices above introduced, a new parameter can be adopted to evaluate the rudder stress and thus the energy consumption. Specifically an index for measuring the action on the rudder is defined as

$$R = \frac{\sum_{t=1}^{T_{\text{tot}}-1} |\Delta\delta(t)|}{L},$$

where $\delta(t)$ is the rudder angle at time t, $\Delta\delta(t) = \delta(t+1) - \delta(t)$, L is the target path length and T_{tot} is obtained by multiplying the sampling rate ($[Hz]$) and the overall experiment duration ($[s]$).

4. LYAPUNOV-BASED VIRTUAL TARGET VS JACOBIAN-BASED PRIORITY TASK APPROACHES

In such a way to prove the effectiveness of the proposed indices, the Charlie USV has been exploited in order to test different navigation, guidance and control architectures; in particular, within the present work, the performances of two different control algorithms are compared, namely the Lyapunov-based virtual target (LBVT) and the Jacobian-based priority task (JBPT) approaches. In the following, these two different control schemes are briefly introduced.

Both the LBVT and the JBPT control schemes exploit a common lower level dynamic control; PI-type linear and angular velocity controllers are designed following a gain-scheduling approach in order to guarantee specific behaviours, in terms of closed-loop characteristic equations. A detailed discussion of the Charlie USV navigation and control system can be found in Caccia et al. [2008a]. The overall software control system relies on a modular architecture, that separates the guidance modules from the lower level controllers (namely speed and yaw rate regulators). This in turn allows to have the exploited kinematic path-following guidance law (LBVT or JBPT) simply feed PI-type (Proportional-Integral) gain-scheduling speed and yaw-rate dynamic controllers.

The LBVT algorithm has been designed and developed following a classical Lyapunov-based method; for details about the kinematic controller design the interested reader can refer to Bibuli et al. [2009], Lapierre and Soetanto [2007] and references therein.

On the other hand, the JBPT scheme exploits the control paradigm of prioritized tasks, usually employed for robotic manipulators. Such a technique allows to obtain an "emergent behaviour" for the robot, while keeping separate the different required actions for the vehicle (e.g. path following and obstacle avoidance), thus providing the ability to add further control tasks easily, without changing the overall architecture. In this case, two simple tasks are considered: the first allows the completion of the path following mission and the other regulates the vehicle velocity. The algorithm is not reported here for sake of brevity but details could be found in Zereik et al. [2013] and Zereik [2013].

5. EXPERIMENTAL SETUP

Both the above suggested algorithms (LBVT and JBPT) have been validated during a test campaign conducted with the Charlie USV. In particular, in the following Subsection 5.1, a brief description of the Charlie USV is provided, while in Subsection 5.2 the introduced performance indices are applied to the obtained experimental data in order to compare the two control schemes.

5.1 Charlie USV

The Charlie USV, depicted in Figure 3, is a small catamaran-like prototype vehicle, originally developed and exploited by the CNR-ISSIA during the XIX Italian expedition to Antarctica in 2003-2004. Its main task regarded the sampling of the sea surface microlayer and the immediate subsurface for the study of the sea-air interaction; for details refer to Caccia et al. [2005].

Charlie is 2.40 m long and 1.70 m wide and its weight in air is about 300 kg. A couple of DC motors (300 W at 48 V) composes the propulsion system and a servoamplifier set provides a PID control of the propeller revolution rates. The vehicle is equipped with a rudder-based steering system: two rigidly connected rudders (placed behind the thrusters) are actuated by a brushless DC motor. The navigation instrumentation set is made up of a GPS Ashtech GG24C integrated with a KVH Azimuth Gyrotrac able to compute true north. Electrical power supply is

Fig. 3. The Charlie USV.

provided by four 12 V at 40 Ah lead batteries integrated with four 32 W triple junction flexible solar panels. The onboard real-time control system, that has been developed using the C++ language, is based on GNU/Linux and runs on a single board computer (SBC), supporting serial and Ethernet communications and PC-104 modules for digital and analog input/output (I/O) (refer to Bruzzone et al. [2008]).

An overview of the Charlie project, including a detailed description of the vehicle and a summary of its applications, can be found in Caccia et al. [2007]. Within such previous works, both kinematics and dynamics have been modelled for the Charlie USV; such models, as well as the nominal values for the parameters of the Charlie USV dynamics can be found in Caccia et al. [2008b].

5.2 Charlie performance

In order to properly compare the JBPT and the LBVT path-following guidance algorithms, different trials have been carried out with Charlie USV:

- 4 tests have been performed adopting the JBPT algorithm for each pair of parameters $(K_\theta, K_u) \in \{(0.2, 0.1); (0.4, 0.2); (0.6, 0.3)\}$, which are the weights of the implemented priority tasks (the interested reader can refer to Zereik [2013]). The JBPT algorithm has been adopted for the first time during this test campaign, for this reason it was not yet optimized. Thus, the performance indices are also exploited in this context to select the best pair of parameters adopted in the implementation of the considered control architecture.
- 4 tests have been completed with the LBVT architecture, for which such tuning was not required during these trials, as it was already accomplished in Bibuli et al. [2009].

All the trials have been performed the same day in few hours and slightly different environmental conditions have been noticed. For the steady state phase, the predefined threshold d has been set to 1 meter, while $\overline{s}$ is equal to 20 seconds.

In Tables 1-3 the JBPT performance indices with their relative mean values for each set of tests are reported for the values $(K_\theta, K_u) \in \{(0.2, 0.1); (0.4, 0.2); (0.6, 0.3)\}$. Analysing Tables 1-2 it is clear that the best path-following precision in both turn and approach phases is achieved when adopting $(K_\theta, K_u) = (0.4, 0.2)$. Table 3 shows that

Table 1. JBPT turn phase indices

JBPT params		Turn		
		$A_1[m^2]$	$H_{1\perp}[m]$	$H_{1\parallel}[m]$
$K_\theta = 0.2$ $K_u = 0.1$	test #1	32.52	7.34	5.18
	test #2	31.65	7.52	4.86
	test #3	24.88	7.82	4.02
	test #4	39.92	7.39	6.21
mean values		**32.24**	**7.52**	**5.07**
$K_\theta = 0.4$ $K_u = 0.2$	test #5	31.18	6.14	5.54
	test #6	23.82	6.21	4.40
	test #7	19.77	6.71	3.68
	test #8	28.77	6.66	4.94
mean values		**25.89**	**6.43**	**4.64**
$K_\theta = 0.6$ $K_u = 0.3$	test #9	28.62	9.05	4.10
	test #10	25.56	6.41	4.74
	test #11	32.72	9.11	4.52
	test #12	72.70	11.73	8.04
mean values		**39.90**	**9.07**	**5.35**

for each trial the settling state phase never occurs and that the best steady state index is reached once more when applying the same values for (K_θ, K_u). Combining the processed data it can be stated that for the JBPT architecture the best performance is obtained when $(K_\theta, K_u) = (0.4, 0.2)$. This is because, even if the $\overline{\chi}$ and R are not the best ones in the tables, the values for the remaining indices are far better than the others; therefore the pair $(0.4, 0.2)$ is also the one selected for the comparison with LBVT in the following.

Figure 4 and Figure 5 show Charlie USV performing trials #1 and #13 reported in Tables 1-6, respectively testing the JBPT and the LBVT approaches. A comparison of the cross-track error evolution, neglecting the turn phase, for both the LBVT and JBPT algorithms is depicted in Figure 6; from the graphs, it can be stated that the LBVT makes the vehicle converge to the path in a faster way and this trend is confirmed by the $\overline{\chi}$ and $\chi_{\max}$ indices' values in Tables 2 and 5. As a remark, it is clear that the analysis of the adopted evaluation indices in Tables 2 and 5 is more precise than the mere graph interpretation.

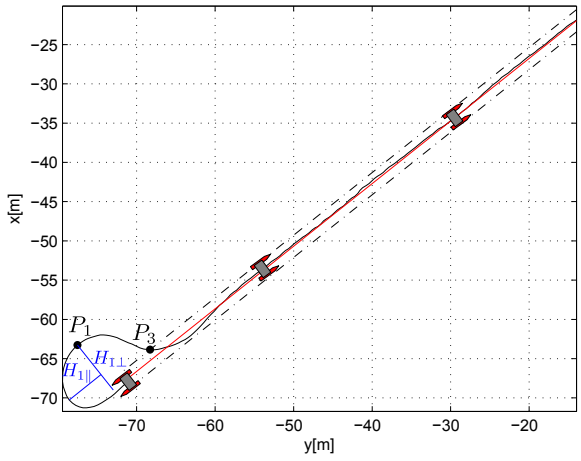

Fig. 4. JBPT path-following along straight line reference (test #1 in Tables 1-3).

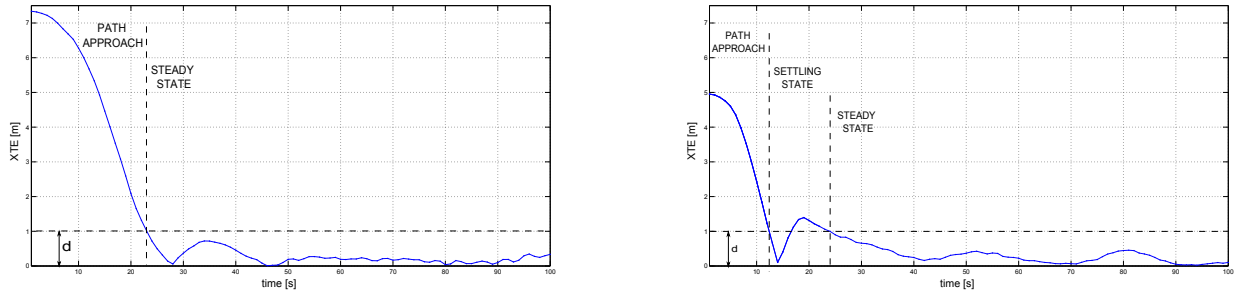

Fig. 6. Comparison of cross-track error evolution excluding the turn phase in JBPT (left) and LBVT (right).

Table 2. JBPT path approach phase indices

JBPT params		Path approach		
		$A_2[m^2]$	$\overline{\chi}[m/s]$	$\chi_{\max}[m/s]$
$K_\theta = 0.2$ $K_u = 0.1$	test #1	36.72	0.29	0.51
	test #2	40.37	0.31	0.50
	test #3	42.92	0.28	0.53
	test #4	38.12	0.31	0.52
mean values		**39.53**	**0.30**	**0.52**
$K_\theta = 0.4$ $K_u = 0.2$	test #5	24.43	0.31	0.54
	test #6	25.24	0.31	0.50
	test #7	25.59	0.32	0.57
	test #8	27.90	0.32	0.53
mean values		**25.79**	**0.32**	**0.53**
$K_\theta = 0.6$ $K_u = 0.3$	test #9	53.17	0.32	0.49
	test #10	24.55	0.32	0.52
	test #11	49.27	0.33	0.48
	test #12	59.46	0.41	0.62
mean values		**46.61**	**0.35**	**0.53**

Table 3. JBPT settling and steady state indices plus rudder stress

JBPT params		Settling state	Steady state	Rudder stress
		$H_2[m]$	$A_3^*[m]$	R[deg/m]
$K_\theta = 0.2$ $K_u = 0.1$	test #1	-	0.21	144.72
	test #2	-	0.19	149.52
	test #3	-	0.23	145.64
	test #4	-	0.18	141.68
mean values		**-**	**0.20**	**145.39**
$K_\theta = 0.4$ $K_u = 0.2$	test #5	-	0.11	118.57
	test #6	-	0.11	115.17
	test #7	-	0.23	118.34
	test #8	-	0.19	123.62
mean values		**-**	**0.16**	**118.93**
$K_\theta = 0.6$ $K_u = 0.3$	test #9	-	0.22	92.38
	test #10	-	0.13	99.45
	test #11	-	0.19	87.80
	test #12	-	0.18	84.72
mean values		**-**	**0.18**	**91.09**

Table 4. LBVT turn phase indices

LBVT params	Turn		
	$A_1[m^2]$	$H_{1\perp}[m]$	$H_{1\parallel}[m]$
test #13	26.37	4.95	6.01
test #14	26.10	7.91	3.98
test #15	30.92	6.06	6.09
test #16	249.32	5.20	4.24
mean values	**83.18**	**6.03**	**5.08**

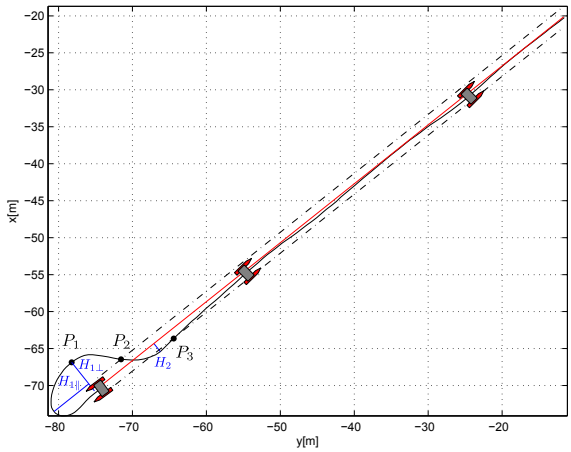

Fig. 5. LBVT path following (with speed adaptation) trial along straight line reference (test #13 in Tables 4-6).

Table 5. LBVT approach phase indices

LBVT params	Approach		
	$A_2[m^2]$	$\overline{\chi}[m/s]$	$\chi_{\max}[m/s]$
test #13	20.06	0.34	0.62
test #14	71.19	0.23	0.54
test #15	29.07	0.31	0.57
test #16	63.50	0.24	0.65
mean values	**45.96**	**0.28**	**0.60**

Table 6. LBVT settling and steady state indices plus rudder stress

LBVT params	Settling state	Steady state	Rudder stress
	$H_2[m]$	$A_3^*[m]$	R[deg/m]
test #13	1.39	0.29	98.23
test #14	-	0.43	101.30
test #15	-	0.17	98.85
test #16	-	0.37	96.19
mean values	**-**	**0.32**	**98.64**

In order to draw a conclusion on the two architectures' performances, it is needed to compare the mean values of the indices reported in Tables 1-6 and to take into account only the case $(K_\theta, K_u) = (0.4, 0.2)$ for the JBPT control scheme. From a quick analysis of the computed mean indices it should be clear that the variance of the values for the LBVT algorithm is quite high (especially regarding

the area indices A_1, A_2 and A_3^*) while the trials with the JBPT lead to more similar results, situation this last that is preferable. Even if there is an evident penalisation on the A_1 index in trial #16 (that can be explained with the robot initial position, as it started farther from the desired path than the other trials), the high variance represents a great disadvantage for the LBVT control scheme. Combining this remark with a comparison of the steady state mean values (0.16 for JBPT vs 0.32 for LBVT) it is obvious that the JBPT scheme results to be better.

6. CONCLUSIONS

The theoretical basis for a preliminary implementation of performance indices to quantitatively measure the performance of a marine robotic system have been addressed in the paper. Many trials have been carried out in Toulon within the EU FP7 project MORPH employing the Charlie USV with the aim to collect experimental data on which computing the formalized indices. This test campaign allowed to evaluate the performance of the JBPT architecture, selecting the best values for its parameters. Moreover, similar experiments were conducted exploiting the LBVT control scheme, allowing to successfully compare the two algorithms. Future research will focus on extending these standards and indices to a more general framework in terms of different tasks and vehicles (such as underwater vehicles). Common criteria should be adopted in a cooperative context in order to effectively assign tasks to different vehicles and this goal can be achieved thanks to the independence of the indices from algorithms and vehicles. Furthermore the development of new performance parameters to evaluate cooperative path-following tasks as well as more general multi-robot systems represents a challenging topic to be addressed in the near future.

REFERENCES

Francesco Amigoni, Simone Gasparini, and Maria Gini. Good experimental methodologies for robotic mapping: A proposal. In *Robotics and Automation, 2007 IEEE International Conference on*, pages 4176–4181. IEEE, 2007.

Francesco Amigoni, Monica Reggiani, and Viola Schiaffonati. An insightful comparison between experiments in mobile robotics and in science. *Autonomous Robots*, 27(4):313–325, 2009.

Steven Balakirsky, Chris Scrapper, Stefano Carpin, and Michael Lewis. Usarsim: providing a framework for multirobot performance evaluation. In *Proceedings of PerMIS*, volume 2006. Citeseer, 2006.

Marco Bibuli, Gabriele Bruzzone, Massimo Caccia, and Lionel Lapierre. Path-following algorithms and experiments for an unmanned surface vehicle. *Journal of Field Robotics*, 26(8):669–688, 2009.

F. Bonsignorio, J. Hallam, and A.P. del Pobil. Good experimental methodology guidelines. Technical report, 2008.

F Bonsignorio, John Hallam, and A del Pobil. Defining the requisites of a replicable robotics experiment. In *RSS2009 Workshop on Good Experimental Methodologies in Robotics*, 2009.

G. Bruzzone, M. Caccia, A. Bertone, and G. Ravera. Standard linux for embedded real-time robotics and manufacturing control systems. *Robotics and Computer Integrated Manufacturing*, 2008. doi: 10.1016/j.rcim.2007.07.016.

M. Caccia, R. Bono, G. Bruzzone, G. Bruzzone, E. Spirandelli, G. Veruggio, A. Stortini, and G. Capodaglio. Sampling sea surface with SESAMO. *Robotics and Automation Magazine*, 12(3):95–105, 2005.

M. Caccia, M. Bibuli, R. Bono, G. Bruzzone, G. Bruzzone, and E. Spirandelli. Unmanned surface vehicle for coastal and protected water applications: The charlie project. *Marine Technology Socety Journal*, 41(2):62–71, 2007.

M. Caccia, M. Bibuli, R. Bono, and G. Bruzzone. Basic navigation, guidance and control of an unmanned surface vehicle. *Autonomous Robots*, 25(4):349–365, 2008a.

M. Caccia, G. Bruzzone, and R. Bono. A practical approach to modeling and identification of small autonomous surface craft. *Journal of Oceanic Engineering*, 2008b. doi: 10.1109/JOE.2008.920157.

M. Caccia, M. Bibuli, G. Bruzzone, and L. Lapierre. Vehicle-following for unmanned surface vehicles. volume 77, pages 201–230. Inst of Engineering & Technology, Control Engineering Series, 2012.

M. Caccia, E. Saggini, M. Bibuli, G. Bruzzone, E. Zereik, and E. Riccomagno. Towards good experimental methodologies for unmanned marine vehicles. *Lecture Notes in Computer Science*, 8112, 2013. in press.

Massimo Caccia, Gabriele Bruzzone, and Riccardo Bono. A practical approach to modeling and identification of small autonomous surface craft. *Oceanic Engineering, IEEE Journal of*, 33(2):133–145, 2008c.

Andrea Caiti. Underwater robot networking: the interplay between communication and cooperation. 2011.

Andreas Fischer, Ching Y Suen, Volkmar Frinken, Kaspar Riesen, and Horst Bunke. A fast matching algorithm for graph-based handwriting recognition. In *Graph-Based Representations in Pattern Recognition*, pages 194–203. Springer, 2013.

L. Lapierre and D. Soetanto. Nonlinear path following control of an auv. *Journal of Oceanic Engineering*, 34: 17341744, 2007.

Nikola Mišković, Zoran Vukić, Marco Bibuli, Gabriele Bruzzone, and Massimo Caccia. Fast in-field identification of unmanned marine vehicles. *Journal of Field Robotics*, 28(1):101–120, 2011.

E. Saggini. Study of the heading parameter in steady-state through repeated medians and correlogram. Master's thesis, University of Genoa, 2012.

Satoshi Tadokoro and Adam Jacoff. Performance metrics for response robots [industrial activities]. *Robotics & Automation Magazine, IEEE*, 18(3):12–14, 2011.

E. Zereik. *Space Robotics Supporting Exploration Missions: Vision, Force Control and Coordination Strategies*. Nova Science Publishers Inc., 2013.

E. Zereik, M. Bibuli, G. Bruzzone, and M. Caccia. Jacobian task priority-based approach for path following of unmanned surface vehicles. In *9th IFAC Conference on Control Applications in Marine Systems (CAMS) 2013*, 2013.

Hu Zhu, Tianxu Zhang, Luxin Yan, and Lizhen Deng. Robust and fast hausdorff distance for image matching. *Optical Engineering*, 51(1):017203–1, 2012.